

Appendix A.51:

Palinurus Rd 2 – CPT 62761

Table 1: Site Description for Palinurus Rd 2 (CPT 62761).

Attribute	Yes/No		Description/Date	Symbol in Figure 1
	10-m Buffer	20-m Buffer		
Near a body of surface water or other free face features?	No	No	The center of the site is ~35 m to the SW from a creek (the free-face height is ~1 m) and ~340 m to the NE from the Heathcote River (the free-face height is ~2.5 m).	NA
Lateral spreading observed during the CES?	No	No	No lateral spreading was observed by the mapping team. ¹	NA
Nearby buildings or structures?	No	No	NA	NA
Sloping land?	No	No	Level ground, open field	NA
Step changes in the ground surface?	No	Yes	Minor vegetated mounds in the NW and SE quadrants of the 20-m buffer.	NA
Retaining walls?	No	No	NA	NA
Vegetation?	No	No	NA	NA
Anthropogenic changes to the site between the LiDAR surveys?	Yes	Yes	Land resurfacing in both buffers between Aug 2014 and Jan 2015.	NA
Other important factors?	Yes	Yes	The paddock is subject to ploughing. Two portable livestock feeders in the NW quadrant of both buffers. Uneven surface with localized areas of tall grass in both buffers.	Feeder: Purple Outline

Note: Buffer is the area within a circle of a specified radius with CPT investigations done at its center (172.689145°, -43.551414°).

¹ Canterbury Geotechnical Database. (2012). "Observed Ground Crack Locations", Map Layer CGD0400 - 23 July 2012, retrieved July 09, 2018 from <https://canterburygeotechnicaldatabase.projectorbit.com/>

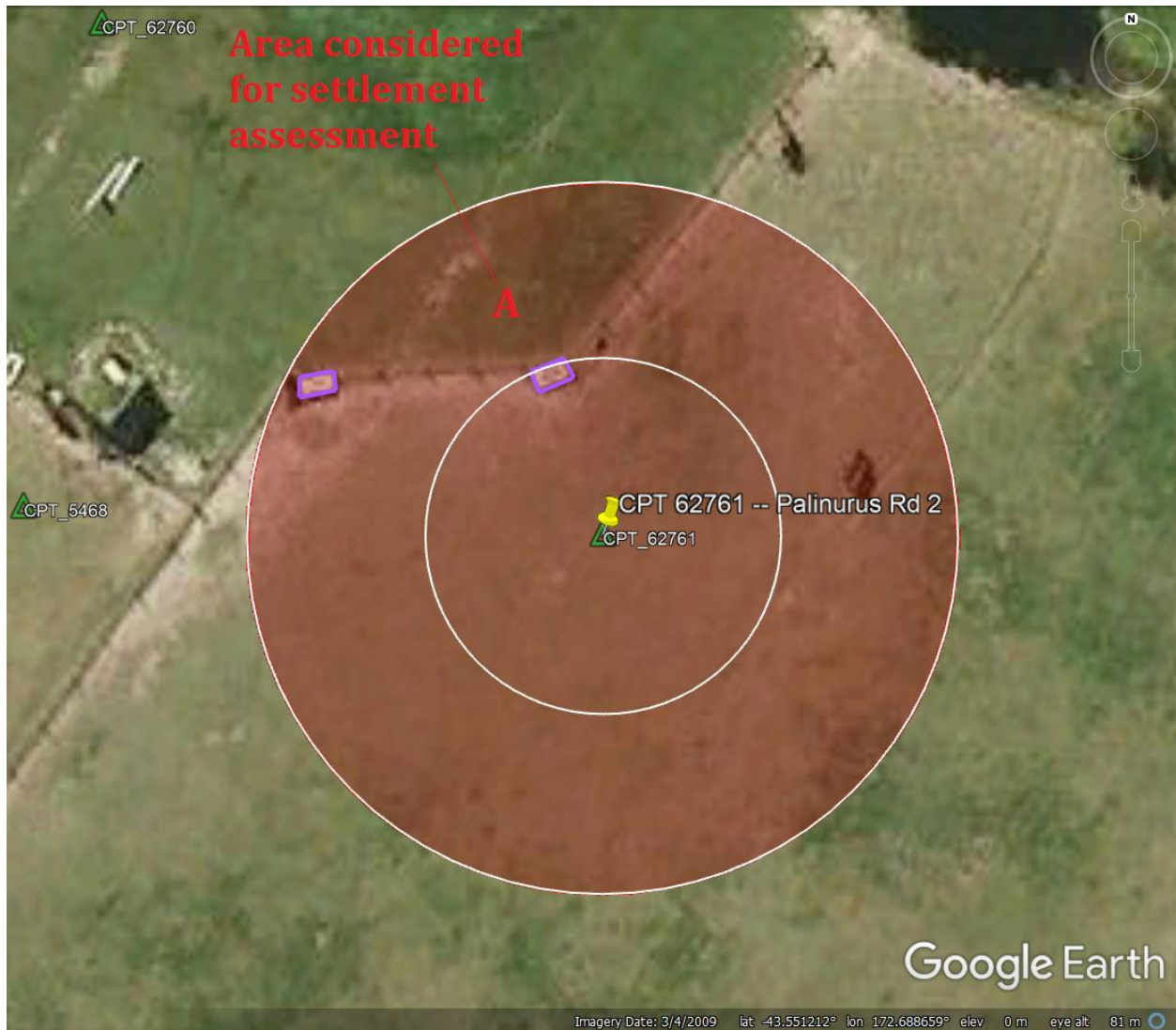


Figure 1: Site plan with areas where ejecta-induced settlement is considered.

Note 1: Patch A in the free field was selected for settlement assessment as an area free of vegetation and structures. Other important factors considered in the patch selection were its proximity to a CPT, a property subjected to addition and/or demolition of a structure, front yard/backyard alterations (e.g., ploughing, rubble, scrap), and aerial distribution of sediment ejecta. The LiDAR-based ejecta-induced settlement analyses were not conducted (please see Tables 1 and 2 for explanation).

Table 2: LiDAR flight error adjustments, global adjustments for the difference between average LiDAR point elevations and benchmark survey elevations, and vertical tectonic movement adjustments.

Earthquake Event(s)	Adjustments (mm)		
	LiDAR Flight Error	Global Offset ²	Tectonic Vertical Movement
Sep-10	NA	-3	0
Feb-11	NA	16	+320
Jun-11	0	38	-30
Dec-11	-50	-65	+25
CES	-50	-14	+315
Any LiDAR survey affected by ejecta?			Yes

Notes: The negative sign indicates the subtraction from the ground surface subsidence, while the positive sign indicates the addition to the ground surface subsidence; Ejecta might have remained on the site at the time of the May 2011 LiDAR survey (ejecta are visible in the 8 Mar 2011 satellite image) and were present at the time of the Sep 2011 LiDAR survey according to the ground photographs from Nov 2011 thus no ejecta-related adjustment is required.

Table 3: LiDAR Measurement Error for Patch A.

Surveys	Buffer	Area Averaged Difference Indicating Repeat Measurement Error (mm)	$\sigma^{*}_{\text{individual LiDAR points}}$ (mm)	%Reduction in σ due to Area Averaging of LiDAR Points
Post Feb 2011: Mar 2011 and May 2011	10-m	ND	59	[ND,ND]
	20-m	ND		
Post Dec 2011: Feb 2012 and Oct 2015	10-m	ND	70	[ND,ND]
	20-m	ND		

*Standard deviation; ND = Not determined.

² Russell, J., & van Ballegooy, S. (2015). *Canterbury Earthquake Sequence: Increased liquefaction vulnerability assessment methodology*. New Zealand: Tonkin & Taylor Ltd.

Table 4: Ground surface subsidence adjustments due to LiDAR measurement error for Patch A.

Earthquake Event(s)	$\sigma_{\text{pre-EQ LiDAR survey}}$ (mm)	$\sigma_{\text{post-EQ LiDAR survey}}$ (mm)	σ_{total} (mm)	Area Average Adjusted σ (mm) **
Sep-10	158	56	134	ND
Feb-11	56	59	59	ND
Jun-11	59	61	62	ND
Dec-11	61	70	87	ND
CES	158	70	124	ND

**Based on the highest %Reduction in Table 3; ND = Not determined due to topographic features.

Table 5: Raw liquefaction-related ground surface subsidence using original LiDAR points for Patch A.

Average Ground Surface Subsidence (mm)		
Earthquake Event(s)	10-m Buffer	20-m Buffer
Sep-10	NA	NA
Feb-11	NA	NA
Jun-11	ND	ND
Dec-11	ND	ND
CES	ND	ND

NA = Not available; ND = Not determined.

Table 6: Corrected liquefaction-related ground surface subsidence using original LiDAR points for Patch A with the calculated adjustments in Table 2.

Average Calculated Ground Surface Subsidence (mm)		
Earthquake Event(s)	10-m Buffer	20-m Buffer
Sep-10	NA	NA
Feb-11	NA	NA
Jun-11	ND	ND
Dec-11	ND	ND
CES	ND	ND

Notes: Plus/minus values are same as those in Table 4a, but rounded to the nearest 25 mm; Positive overall values indicate ground surface subsidence, while negative overall values indicate ground surface uplift; NA = Not available; ND = Not determined.

Table 7: Corrected liquefaction-related ground surface subsidence for Patch A using LiDAR DEMs.

Earthquake Event(s)	Estimated Ground Surface Subsidence (mm)					
	10-m Buffer			20-m Buffer		
	16 th %ile	50 th %ile	84 th %ile	16 th %ile	50 th %ile	84 th %ile
Sep-10	NA	NA	NA	NA	NA	NA
Feb-11	NA	NA	NA	NA	NA	NA
Jun-11	<50	50	50	<50	50	50
Dec-11	<50	<50	<50	<50	<50	<50
CES	50	100	100	50	100	100

Note: These percentiles are not the exact statistical measures; they indicate the spatial variability of ground surface subsidence; NA = Not available

Table 8a: Ejecta-Induced settlement for the top 20 m of the soil profile for Patch A (10-m buffer) for the 50th %ile PGA, $P_L=50\%$, and $C_{FC}=0.13$ using BI-2014, ZRB-2002, and I_c cutoff of 2.6.

Earthquake Event(s)	M_W	PGA (g)	Depth to Groundwater (m)	S_T (mm)	S_{V1D} (mm)	$S_{E,L}$ (mm)
Sep-10	7.1	0.24	0.9	NA	116 ± 20	NA
Feb-11	6.2	0.68	0.8	NA	269 ± 50	NA
Jun-11	6.2	0.42	0.9	ND	200 ± 25	ND
Dec-11	6.1	0.29	1.3	ND	94 ± 50	ND

Notes: S_T = Total settlement (Table 6); S_{V1D} = Average vertical settlement due to volumetric compression using Boulanger and Idriss (2014) (BI-2014), Zhang et al. (2002) (ZRB-2002) procedures and de Greef and Lengkeek (2018) thin-layer correction; $S_{E,L}$ = Ejecta-induced settlement as the difference between the LiDAR-based S_T and S_{V1D} ; NA = Not available; ND = Not determined.

Table 8b: Ejecta-Induced settlement for the top 20 m of the soil profile for Patch A (20-m buffer) for the 50th %ile PGA, $P_L=50\%$, and $C_{FC}=0.13$ using BI-2014, ZRB-2002, and I_c cutoff of 2.6.

Earthquake Event(s)	M_W	PGA (g)	Depth to Groundwater (m)	S_T (mm)	S_{V1D} (mm)	$S_{E,L}$ (mm)
Sep-10	7.1	0.24	0.9	NA	116 ± 20	NA
Feb-11	6.2	0.68	0.8	NA	269 ± 50	NA
Jun-11	6.2	0.42	0.9	ND	200 ± 25	ND
Dec-11	6.1	0.29	1.3	ND	94 ± 50	ND

Notes: S_T = Total settlement (Table 6); S_{V1D} = Average vertical settlement due to volumetric compression using Boulanger and Idriss (2014) (BI-2014), Zhang et al. (2002) (ZRB-2002) procedures and de Greef and Lengkeek (2018) thin-layer correction; $S_{E,L}$ = Ejecta-induced settlement as the difference between the LiDAR-based S_T and S_{V1D} ; NA = Not available; ND = Not determined.

Note 2: The uncertainty for volumetric settlement was derived based on the sensitivity of volumetric settlement to PGA, C_{FC} , and P_L for each earthquake event for VsVp 57203 *Shirley Intermediate School* and CC LIQ 1 – CPT 5586 – *Vivian St* sites. Taking the 50th percentile as the baseline case, the minimum and maximum values corresponding to the difference between the 25th percentile and the 50th percentile and the 75th percentile and the 50th percentile were determined. The arithmetic mean of the range of the minimum and maximum difference was evaluated for each patch at the two sites. The maximum arithmetic mean for each earthquake event was rounded to the nearest five and used as the uncertainty value. Accordingly, the 1-D volumetric settlement uncertainties of ± 20 , ± 50 , ± 25 , and ± 50 mm for the Sep-10, Feb-11, Jun-11, and Dec-11 earthquake events, respectively, were used for all sites in this study.

Table 9a: Coverage area and height of ejecta estimates for Patch A (10-m buffer) using photographs.

EQ Event	$A_{E,thick1}$ (m ²)	$H_{E,thick1}$ (m)	$A_{E,thick2}$ (m ²)	$H_{E,thick2}$ (m)	$A_{E,thin1}$ (m ²)	$H_{E,thin1}$ (m)	$A_{E,thin2}$ (m ²)	$H_{E,thin2}$ (m)	$A_{E,thin3}$ (m ²)	$H_{E,thin3}$ (m)	A_T (m ²)
Sep-10	0	0	0	0	0	0	0	0	0	0	314
Feb-11	73.7	120-180	42.2	80-140	27.4	60-100	29.7	10-20	94.4	3-6	313*
Jun-11	0	0	28.1	60-120	89.3	40-60	80.0	20-30	0	0	313*
Dec-11	0	0	0	0	0	0	0	0	0	0	314

Notes: $A_{E,thick/thin}$ = Coverage area of thick/thin ejecta layers; $H_{E,thick/thin}$ = Lower-upper estimate of height of thick/thin ejecta layers; A_T = Total assessment area of a buffer being considered; Thin and thick layers correspond to light gray and dark gray colors of ejecta observed in aerial photographs; * indicates reduction in A_T due to the presence of objects.

Table 9b: Coverage area and height of ejecta estimates for Patch A (20-m buffer) using photographs.

EQ Event	$A_{E,thick1}$ (m ²)	$H_{E,thick1}$ (m)	$A_{E,thick2}$ (m ²)	$H_{E,thick2}$ (m)	$A_{E,thin1}$ (m ²)	$H_{E,thin1}$ (m)	$A_{E,thin2}$ (m ²)	$H_{E,thin2}$ (m)	$A_{E,thin3}$ (m ²)	$H_{E,thin3}$ (m)	A_T (m ²)
Sep-10	0	0	0	0	0	0	0	0	0	0	1257
Feb-11	125	120-180	81.1	80-140	139	60-100	237	10-20	286	3-6	1253*
Jun-11	0	0	128	60-120	223	40-60	465	20-30	0	0	1252*
Dec-11	0	0	0	0	0	0	0	0	0	0	1257

Notes: $A_{E,thick/thin}$ = Coverage area of thick/thin ejecta layers; $H_{E,thick/thin}$ = Lower-upper estimate of height of thick/thin ejecta layers; A_T = Total assessment area of a buffer being considered; Thin and thick layers correspond to light gray and dark gray colors of ejecta observed in aerial photographs; * indicates reduction in A_T due to the presence of objects.

Note 3: The values in Table 9 correspond to the coverage area of ejecta outlined in aerial photographs (Figures 8, 9, 19, 19, 35, and 36) and the lower and upper estimates of ejecta height based on geometrical approximations, ground photographs (Figures 38 and 39), and EQC LDAT property inspection reports (e.g., Figure 37). The ejecta-induced settlement using photographs and engineering judgment, $S_{E,P}$, is estimated as

$$S_{E,P} = \frac{\sum_{i=1}^a A_{E,thick,i} * H_{E,thick,i} + \sum_{j=1}^b A_{E,thin,j} * H_{E,thin,j}}{A_T} = \frac{\sum_{i=1}^a V_{E,thick,i} + \sum_{j=1}^b V_{E,thin,j}}{A_T}$$

where

- $A_{E,thick,i}$ and $H_{E,thick,i}$ are the area and the height, respectively, of a thick ejecta layer;
- $A_{E,thin,j}$ and $H_{E,thin,j}$ are the area and the height, respectively, of a thin ejecta layer;
- A_T is the total assessment area for a buffer being considered (Figure 1).

Table 10: Ejecta-induced settlement estimates for Patch A based on photographs.

Earthquake Event	Patch A (10-m buffer)		Patch A (20-m buffer)	
	$SE_{P,lower}$ (mm)	$SE_{P,upper}$ (mm)	$SE_{P,lower}$ (mm)	$SE_{P,upper}$ (mm)
Sep-10	0	0	0	0
Feb-11	46	74	26	43
Jun-11	22	36	21	34
Dec-11	0	0	0	0

Note: $SE_{P,lower}$ and $SE_{P,upper}$ correspond to lower and upper estimates of $SE_{P,}$ respectively.

Table 11: Best final estimates of ejecta-induced settlement for Patch A.

EQ Event	Patch A (10-m buffer)			Patch A (20-m buffer)		
	$SE_{E,L}$ (mm)	$SE_{E,P}$ (mm)	$SE_{E,final}$ (mm)	$SE_{E,L}$ (mm)	$SE_{E,P}$ (mm)	$SE_{E,final}$ (mm)
Sep-10	NA	0	0	NA	0	0
Feb-11	NA	60±14	60±15	NA	35±8	35±10
Jun-11	ND	29±7	30±5	ND	28±6	30±5
Dec-11	ND	0	0	ND	0	0

Notes: $SE_{E,L}$ = Ejecta-induced settlement based on LiDAR data reported in Table 8; $SE_{E,P}$ = Median ejecta-induced settlement for the range of values reported in Table 10; $SE_{E,final}$ = Best final estimate of ejecta-induced settlement rounded to the nearest 5 mm; Final plus/minus values are also rounded to the nearest 5 mm.

Note 4:

- $SE_{E,final}$ for Patch A is based solely on $SE_{E,P}$ for all earthquake events.
- The Palinurus Rd 2 site is in the zone of slight to moderate LPI overprediction of liquefaction severity for the Sep-10 EQ and moderate to severe LPI overprediction of liquefaction severity for the Feb-11 EQ (Maurer et al. 2014³). The LDAT inspection reports and ground photographs from Nov 2011 are available for almost all surrounding properties. The ejecta height at the inspected properties was not measured.

³ Maurer, B. W., Green, R. A., Cubrinovski, M., & Bradley, B. A. (2014). Evaluation of the Liquefaction Potential Index for Assessing Liquefaction Hazard in Christchurch, New Zealand. *Journal of Geotechnical and Geoenvironmental Engineering*, 140(7), 04014032-1-11. doi:10.1061/(asce)gt.1943-5606.0001117

Summary 1:

The best estimate of the ejecta-induced free-field ground settlement at the Palinurus Rd site for the SEP 2010, FEB 2011, JUN 2011, and DEC 2011 earthquake is 0 mm, 35 ± 10 mm, 30 ± 5 mm, and 0 mm, respectively.

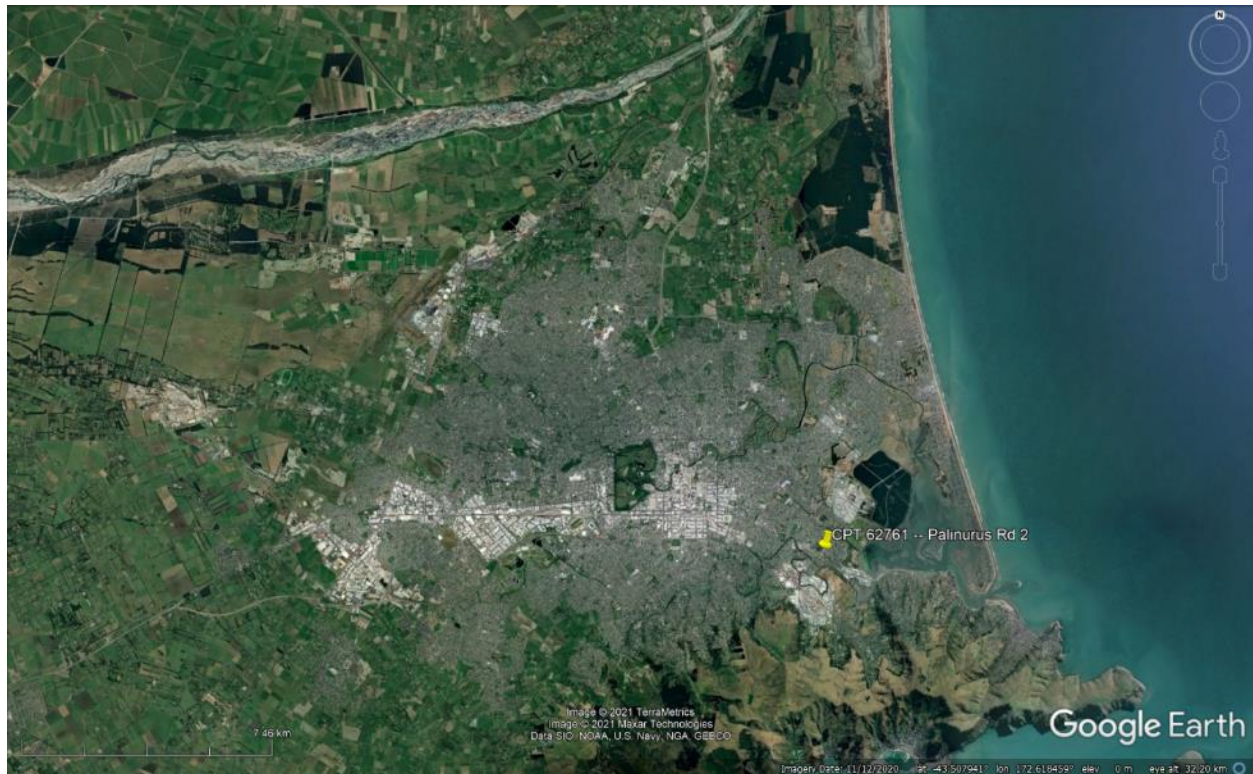


Figure 2: Location of the site.

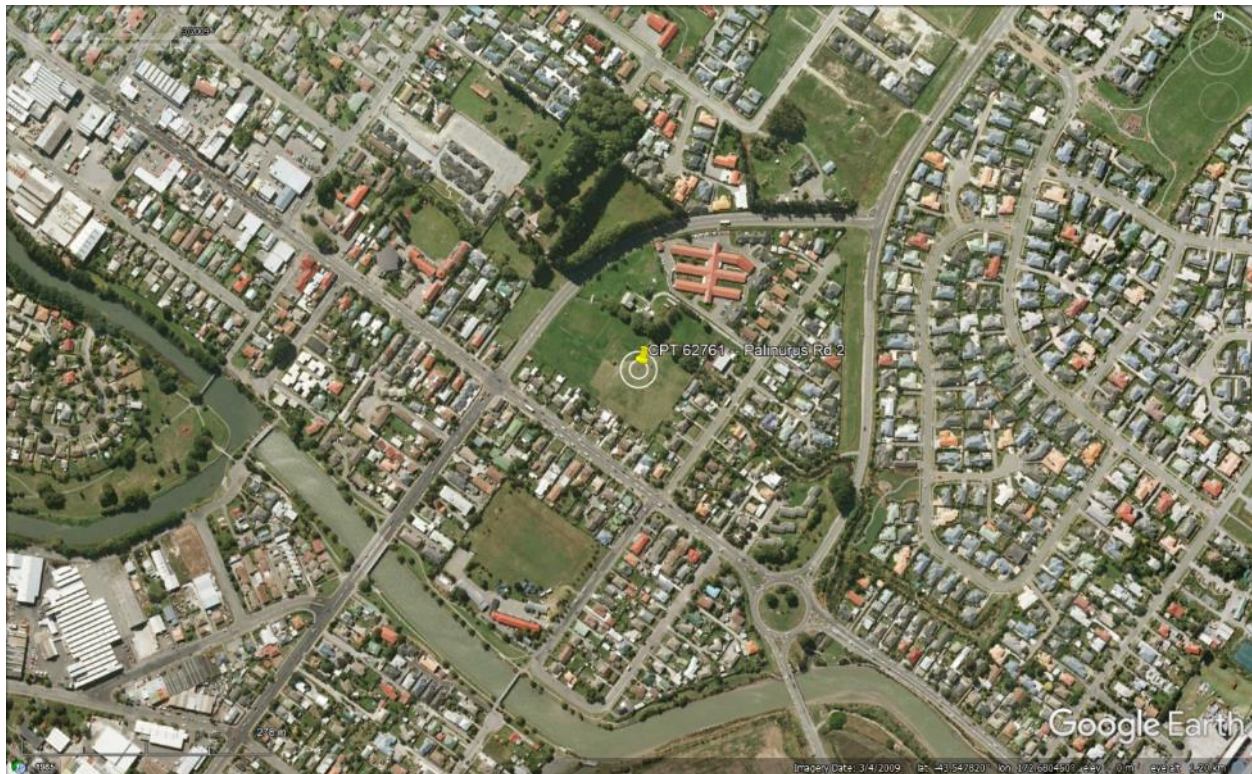


Figure 3: Position of the site relative to nearby buildings, vegetation, and free-face features.



Figure 4: Street view of the level site (the area behind the shed).

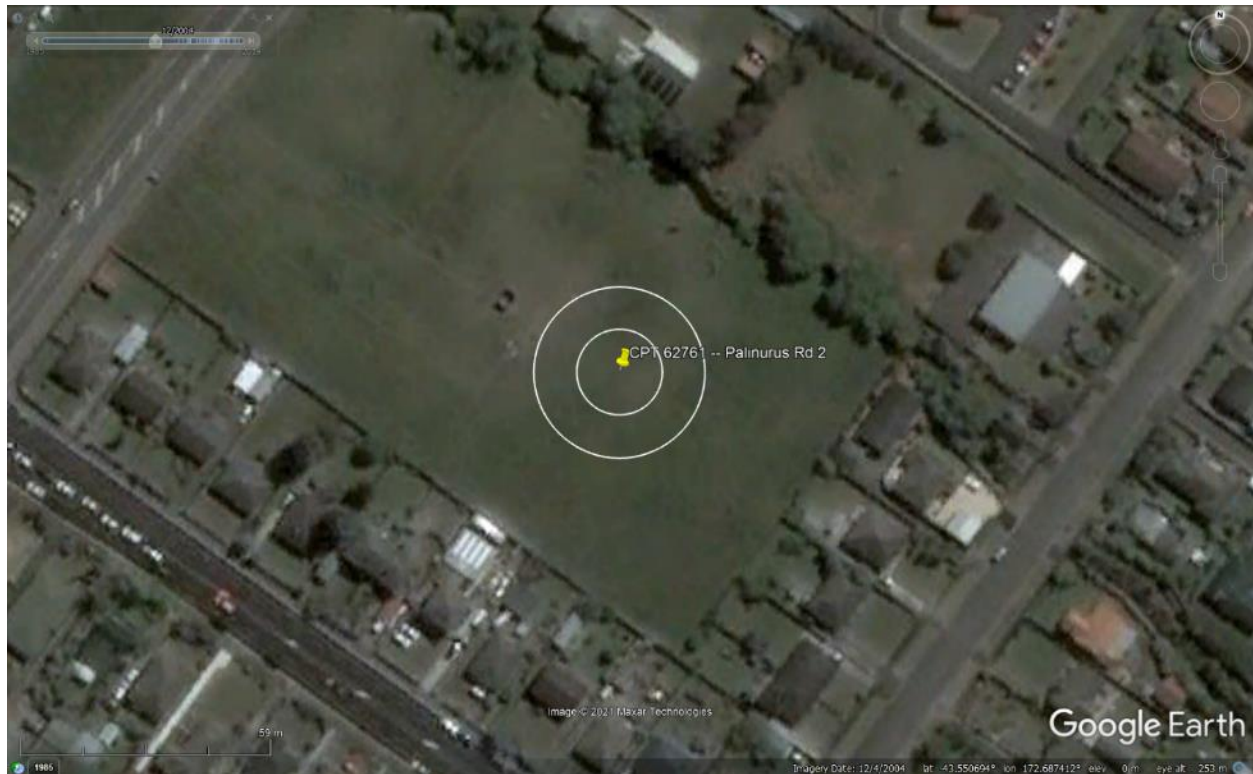


Figure 5: Satellite image of the site taken in Dec 2004.

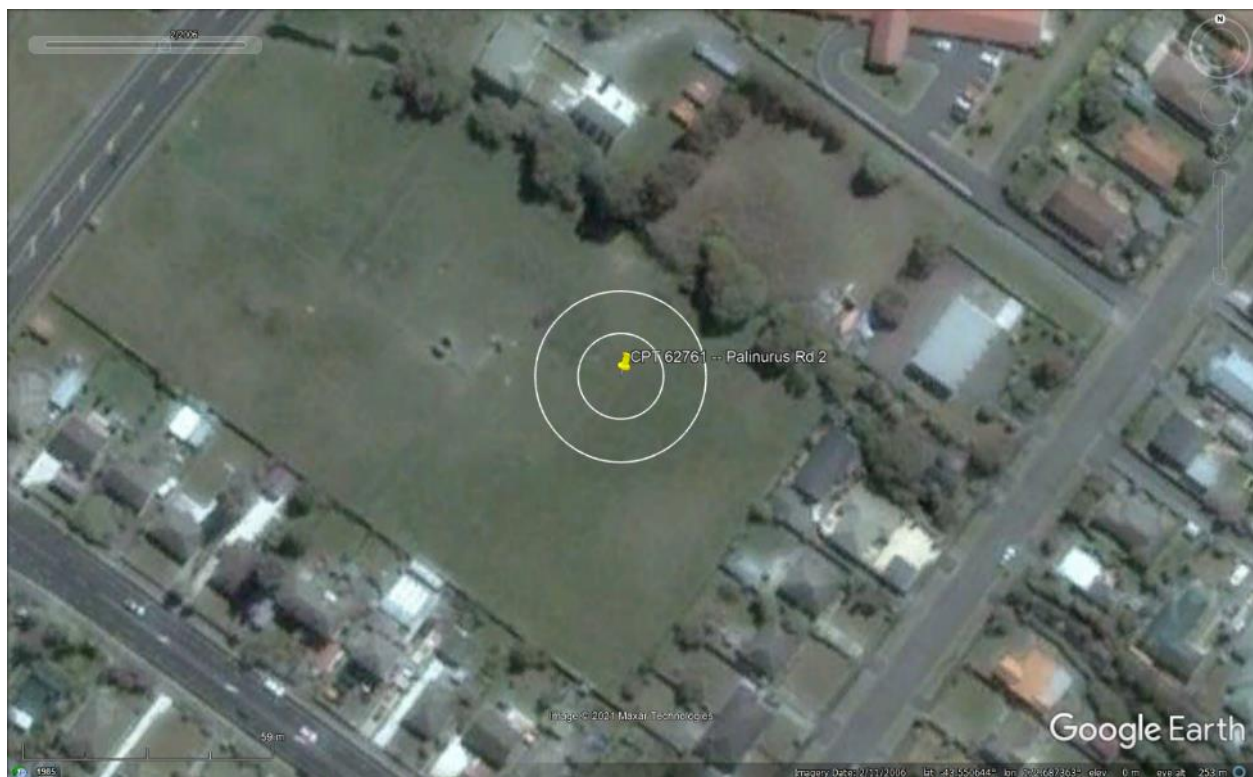


Figure 6: Satellite image of the site taken in Feb 2006.



Figure 7: Satellite image of the site taken in Mar 2009.



Figure 8: Satellite image of the site taken on Sep 3, 2010.



Figure 9: Satellite image of the site taken on Sep 5, 2010.



Figure 10: Satellite image of the site taken on Feb 15, 2011.

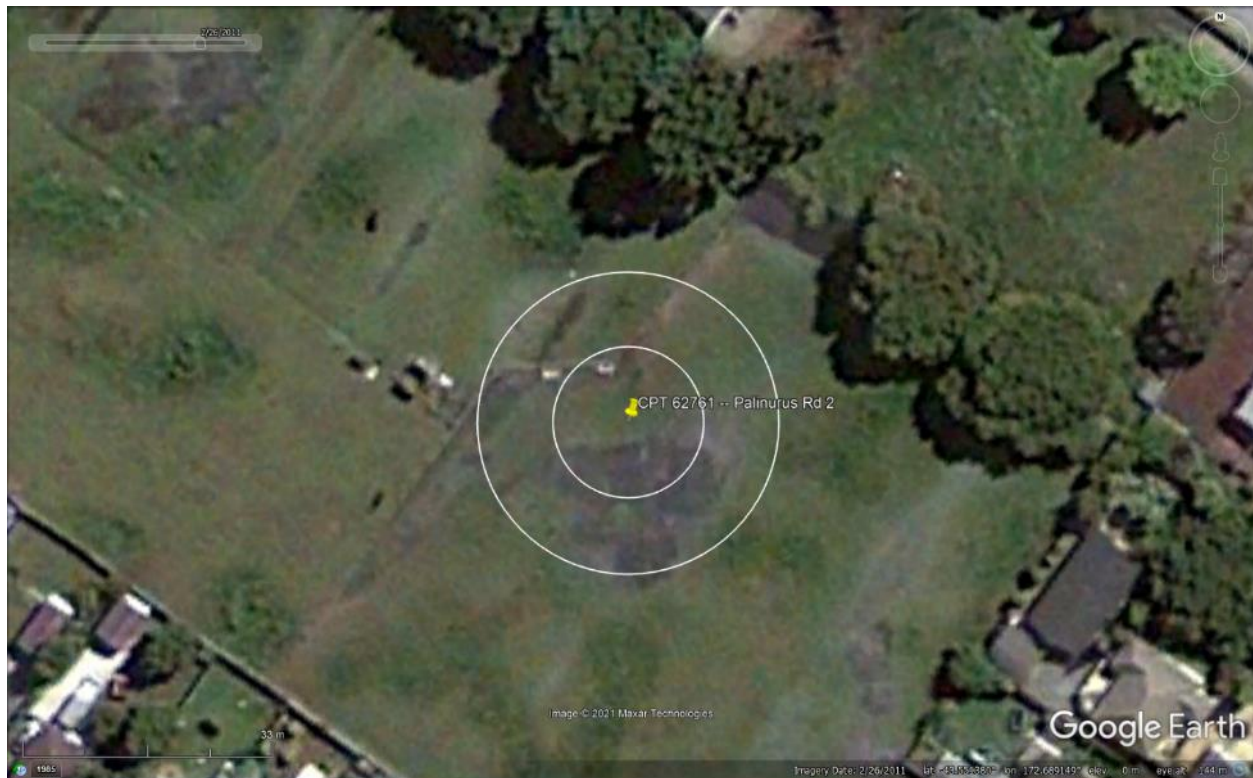


Figure 11: Satellite image of the site taken on Feb 26, 2011.



Figure 12: Satellite image of the site taken on Mar 8, 2011.



Figure 13: Satellite image of the site taken in Apr 2012.

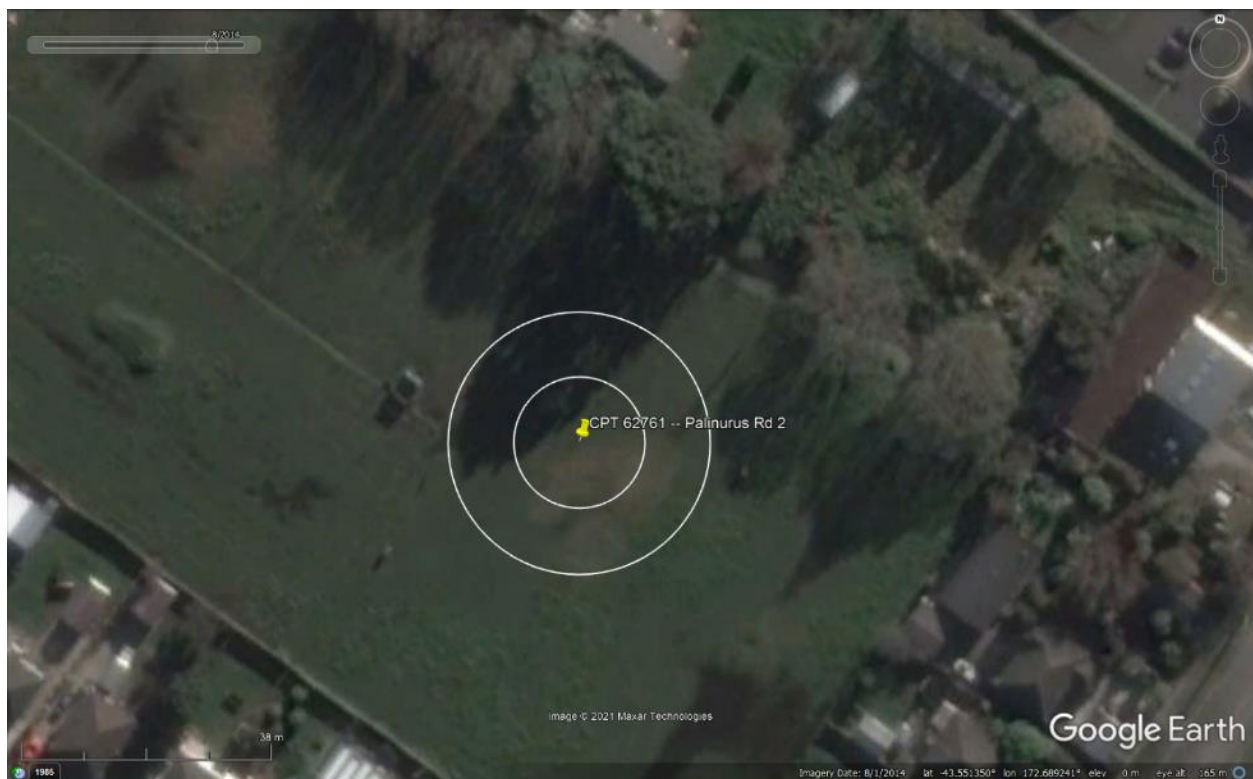


Figure 14: Satellite image of the site taken in Aug 2014.

Liquefaction Ejecta Case Histories for 2010-11 Canterbury Earthquakes

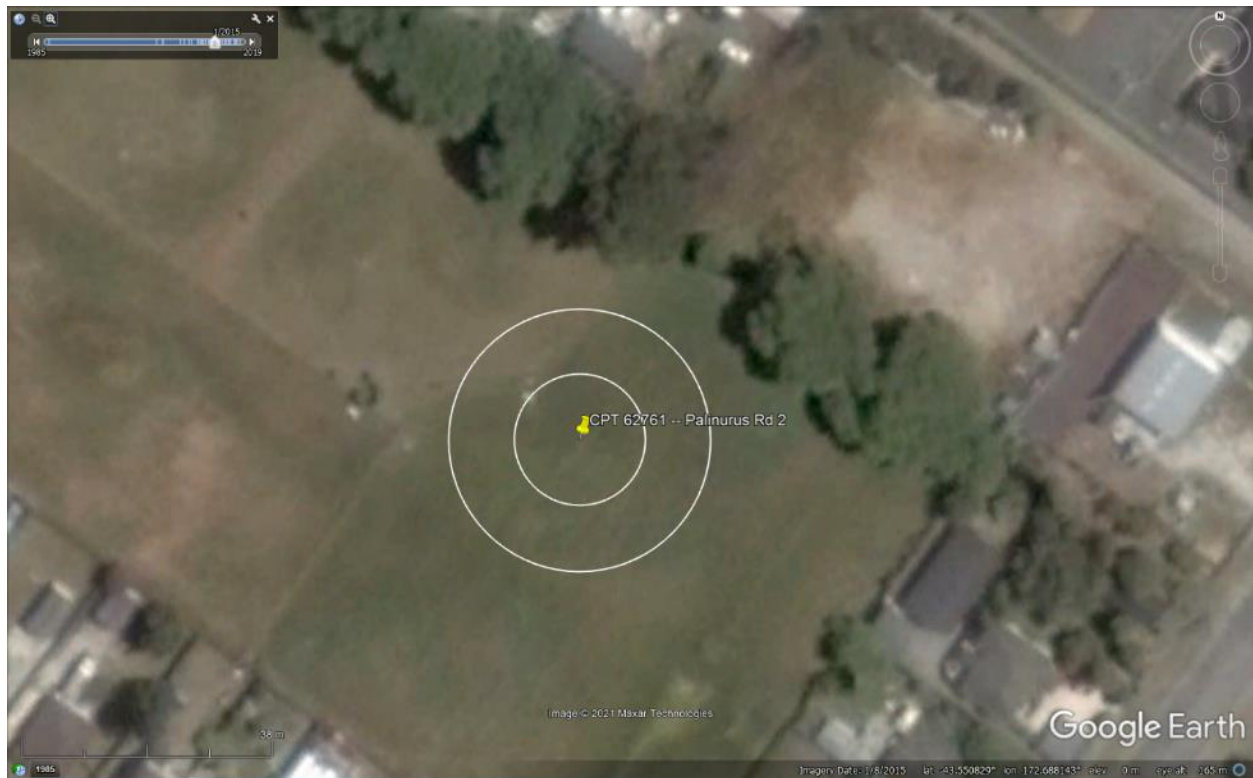


Figure 15: Satellite image of the site taken in Jan 2015.



Figure 16: Satellite image of the site taken in Nov 2015.

Liquefaction Ejecta Case Histories for 2010-11 Canterbury Earthquakes



Figure 17: Aerial photograph from Sep 4, 2010, is not available for the site.



Figure 18: Aerial photograph of the site taken on Feb 24, 2011.

Liquefaction Ejecta Case Histories for 2010-11 Canterbury Earthquakes



Figure 19: Aerial photograph of the site taken on June 14-15, 2011.



Figure 20: Aerial photograph of the site taken on June 16, 2011.

Liquefaction Ejecta Case Histories for 2010-11 Canterbury Earthquakes



Figure 21: Aerial photograph of the site taken on Dec 24, 2011.

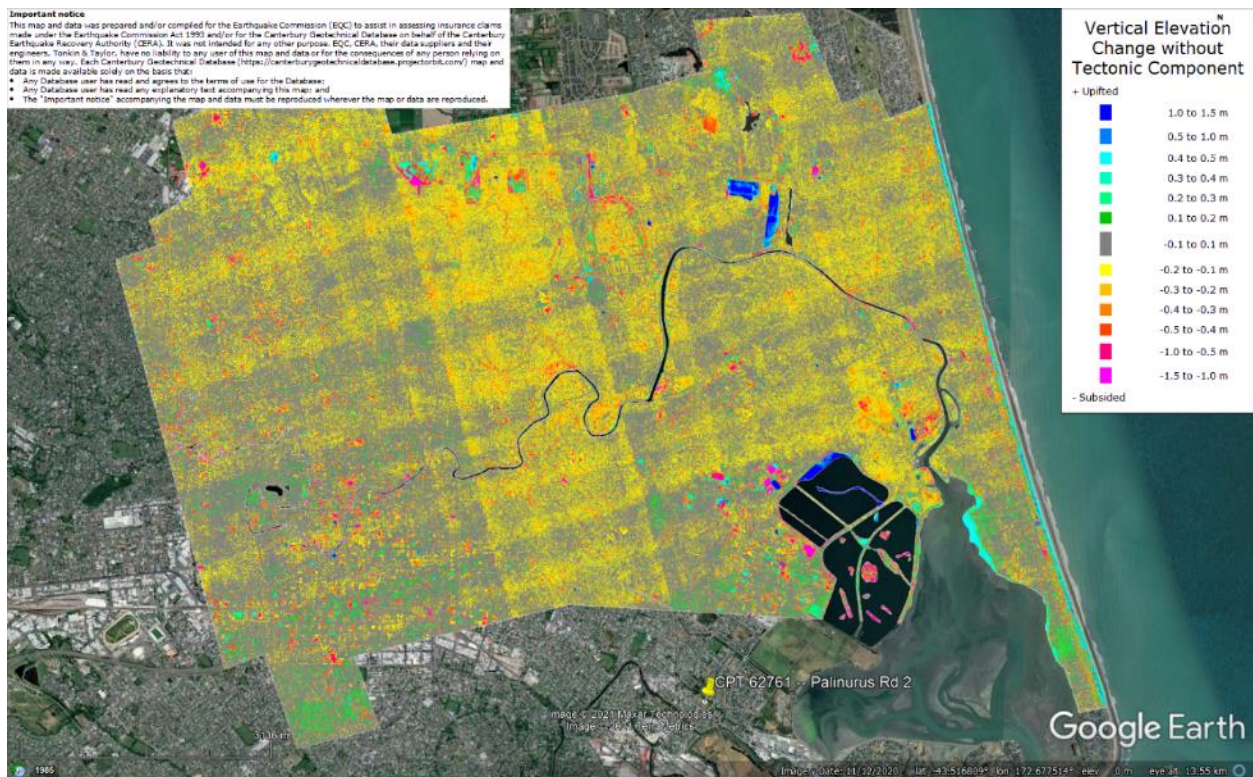


Figure 22: Vertical Ground Movements (Surface – Tectonic) for Sep 2010 Earthquake are not available for the site.

Liquefaction Ejecta Case Histories for 2010-11 Canterbury Earthquakes

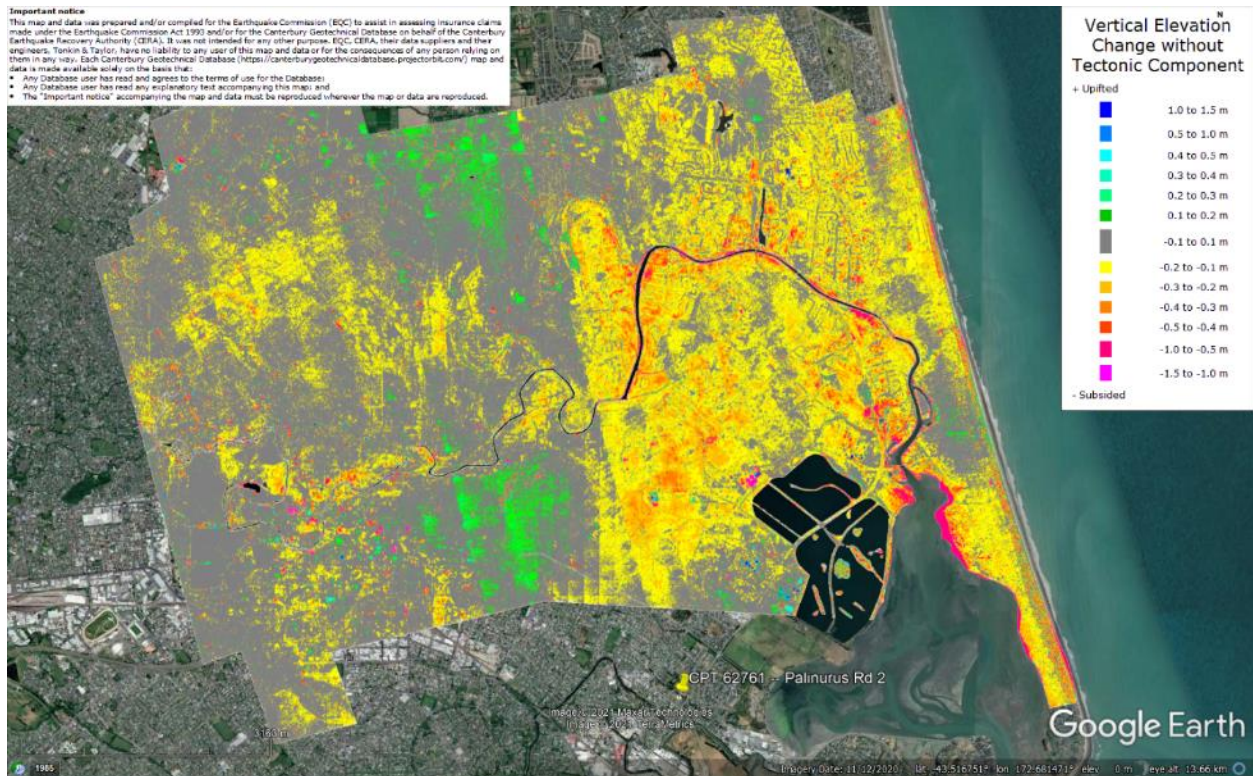


Figure 23: Vertical Ground Movements (Surface – Tectonic) for Feb 2011 Earthquake are not available for the site.

Liquefaction Ejecta Case Histories for 2010-11 Canterbury Earthquakes

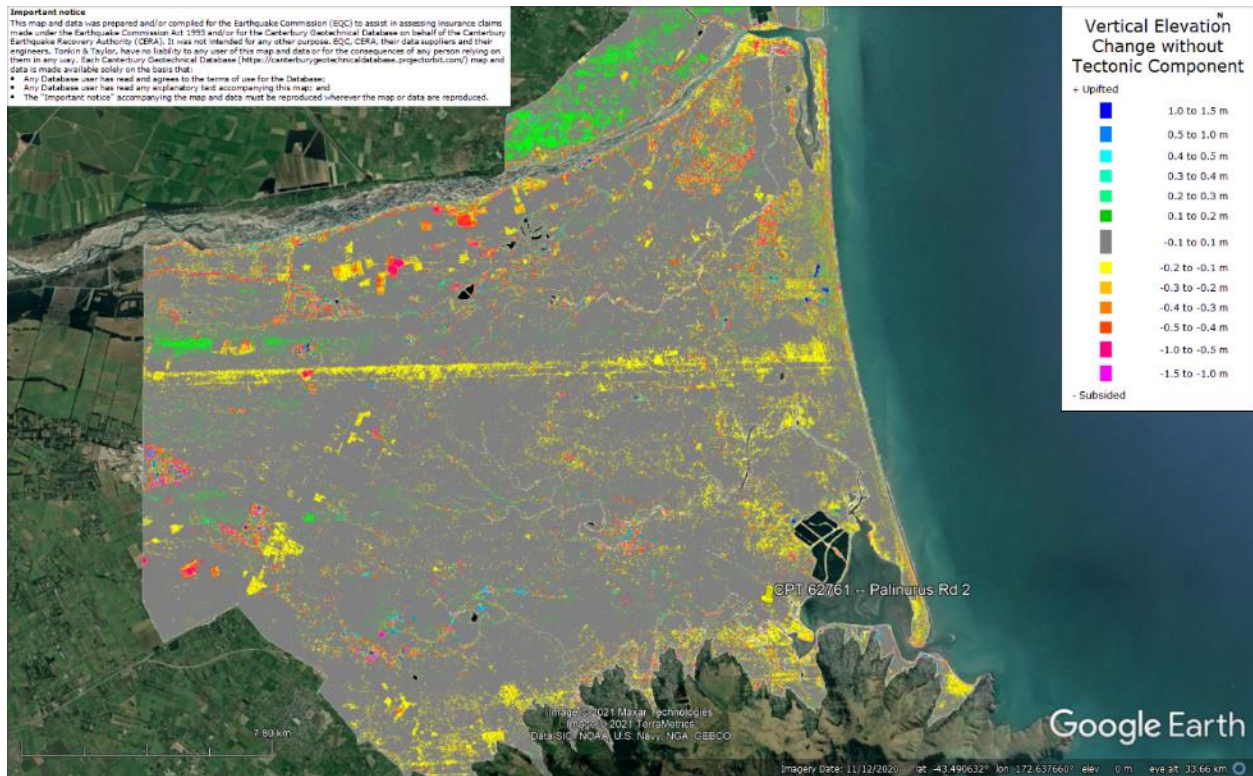


Figure 24: Vertical Ground Movements (Surface – Tectonic) for June 2011 Earthquake – the site is not in the apparent zone of overestimated ground surface subsidence.

Liquefaction Ejecta Case Histories for 2010-11 Canterbury Earthquakes

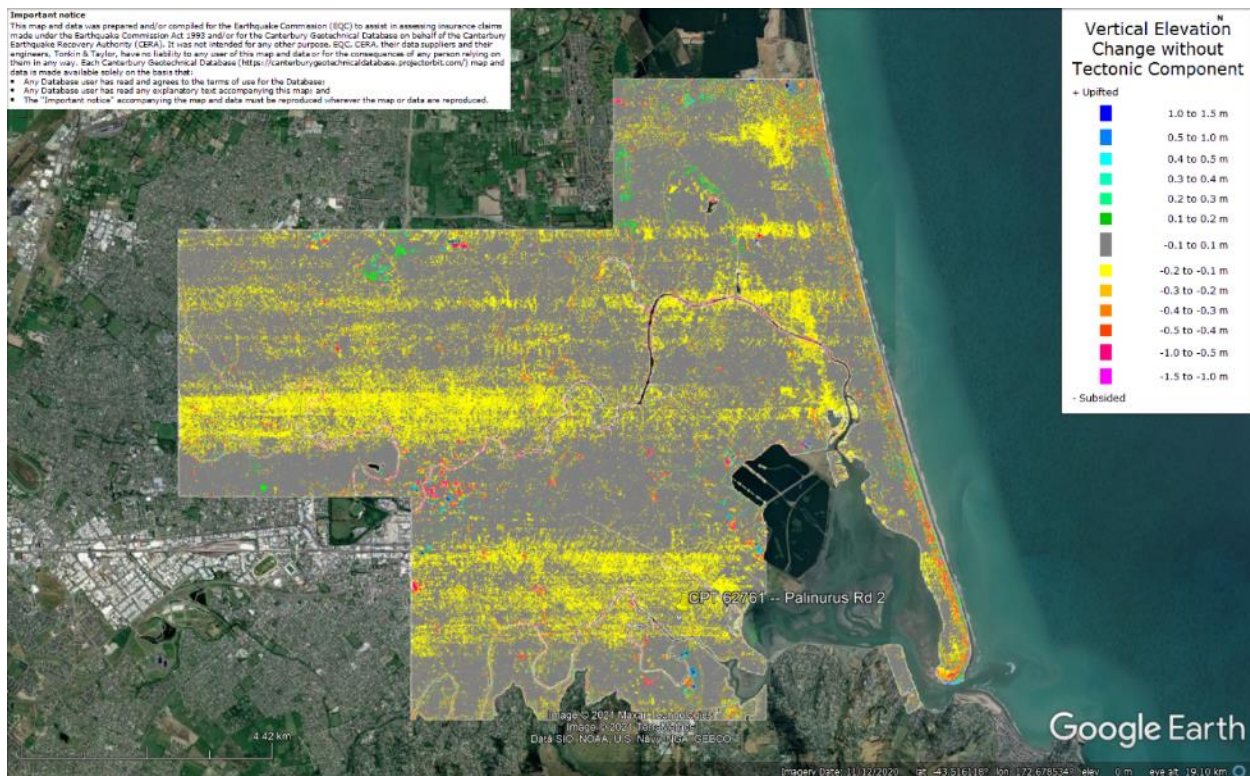


Figure 25: Vertical Ground Movements (Surface – Tectonic) for Dec 2011 Earthquake – the site is in the apparent zone of overestimated ground surface subsidence (i.e., Feb 2012 LiDAR flight error).

Liquefaction Ejecta Case Histories for 2010-11 Canterbury Earthquakes

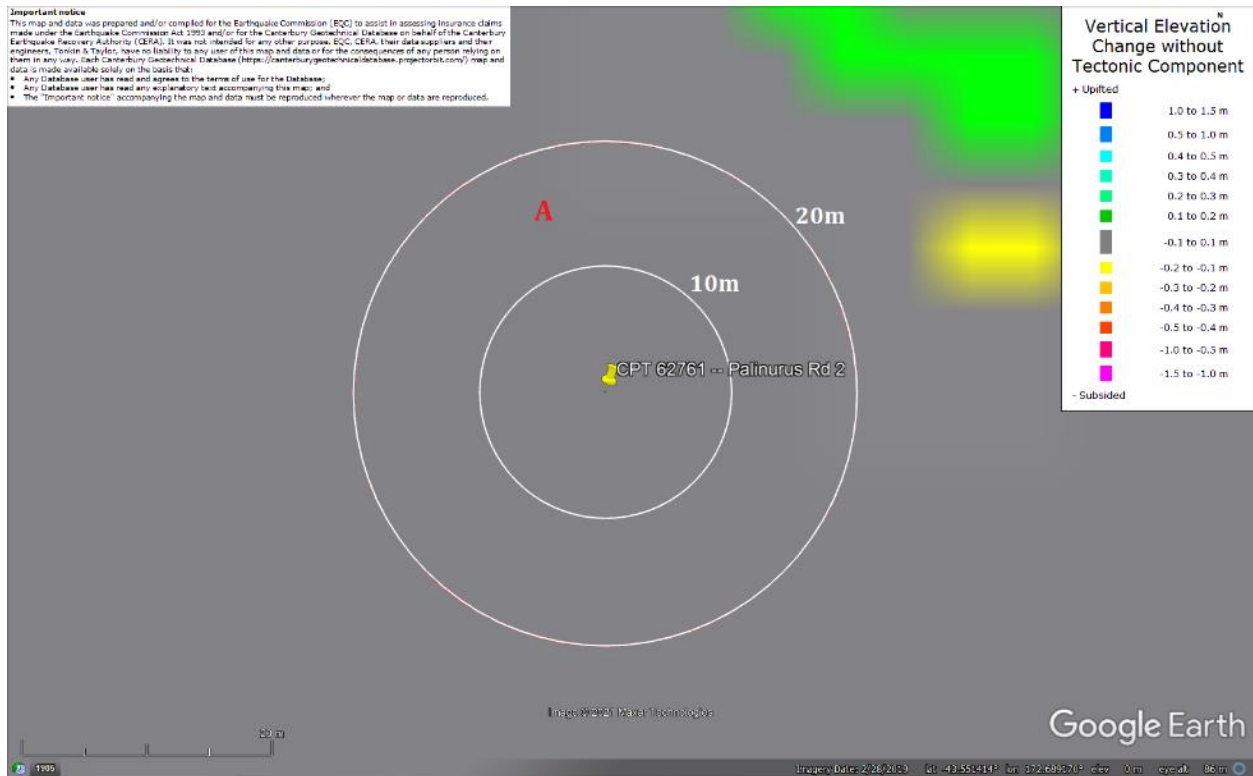


Figure 26: Ground surface subsidence without tectonic component for June 2011 Earthquake according to the LiDAR DEM.

Liquefaction Ejecta Case Histories for 2010-11 Canterbury Earthquakes

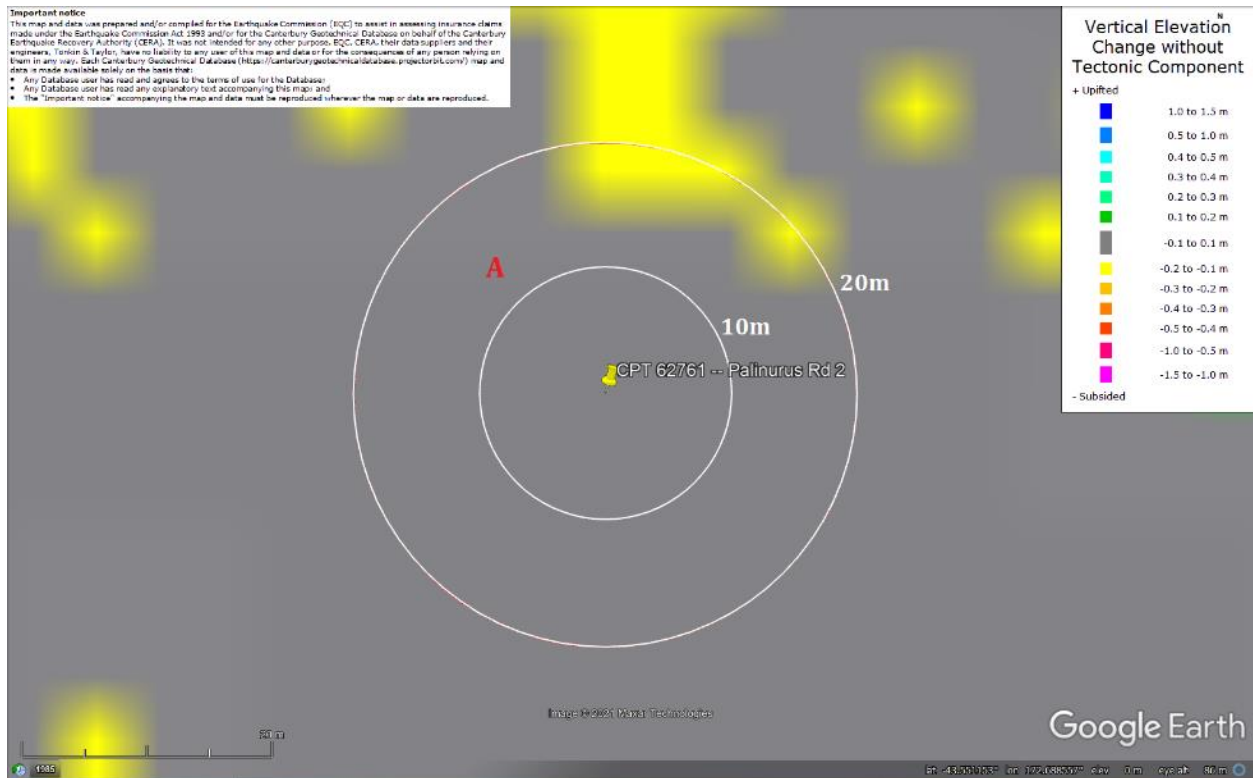


Figure 27: Ground surface subsidence without tectonic component for Dec 2011 Earthquake according to the LiDAR DEM.

Liquefaction Ejecta Case Histories for 2010-11 Canterbury Earthquakes

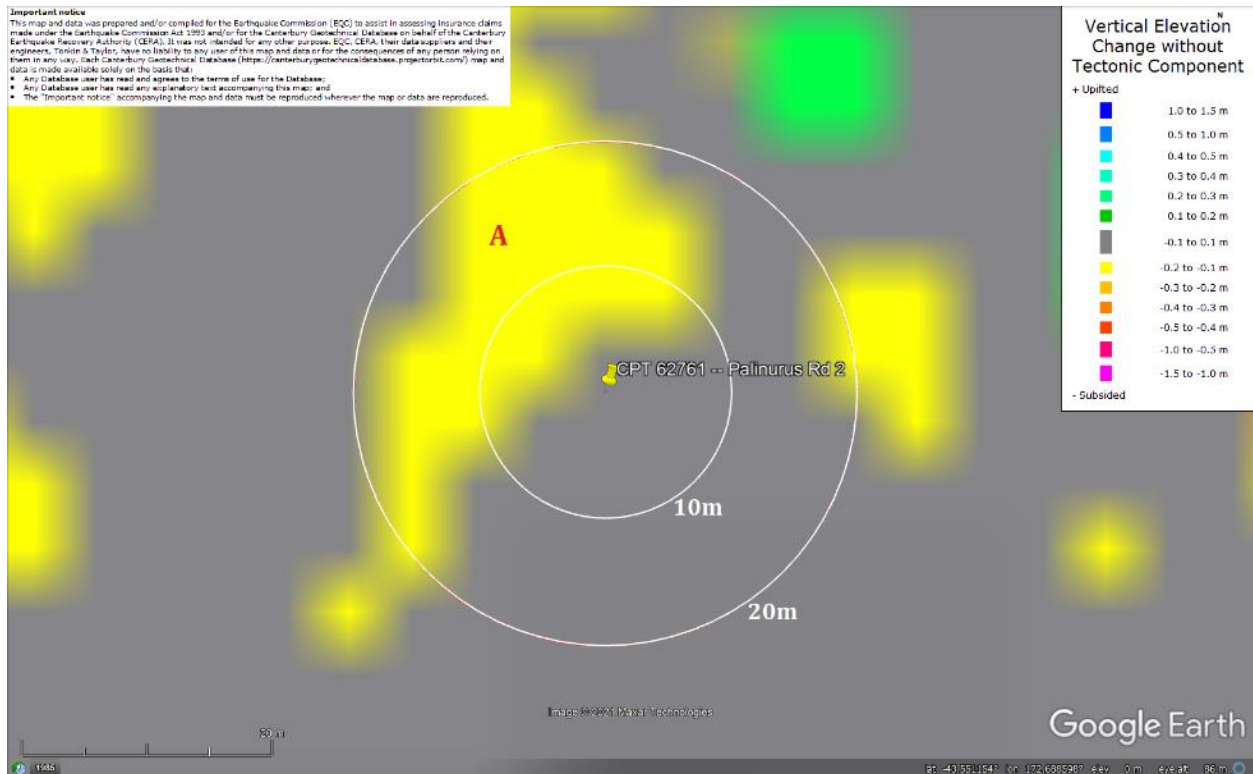


Figure 28: Ground surface subsidence without tectonic component for Canterbury Earthquake Sequence according to the LiDAR DEM.

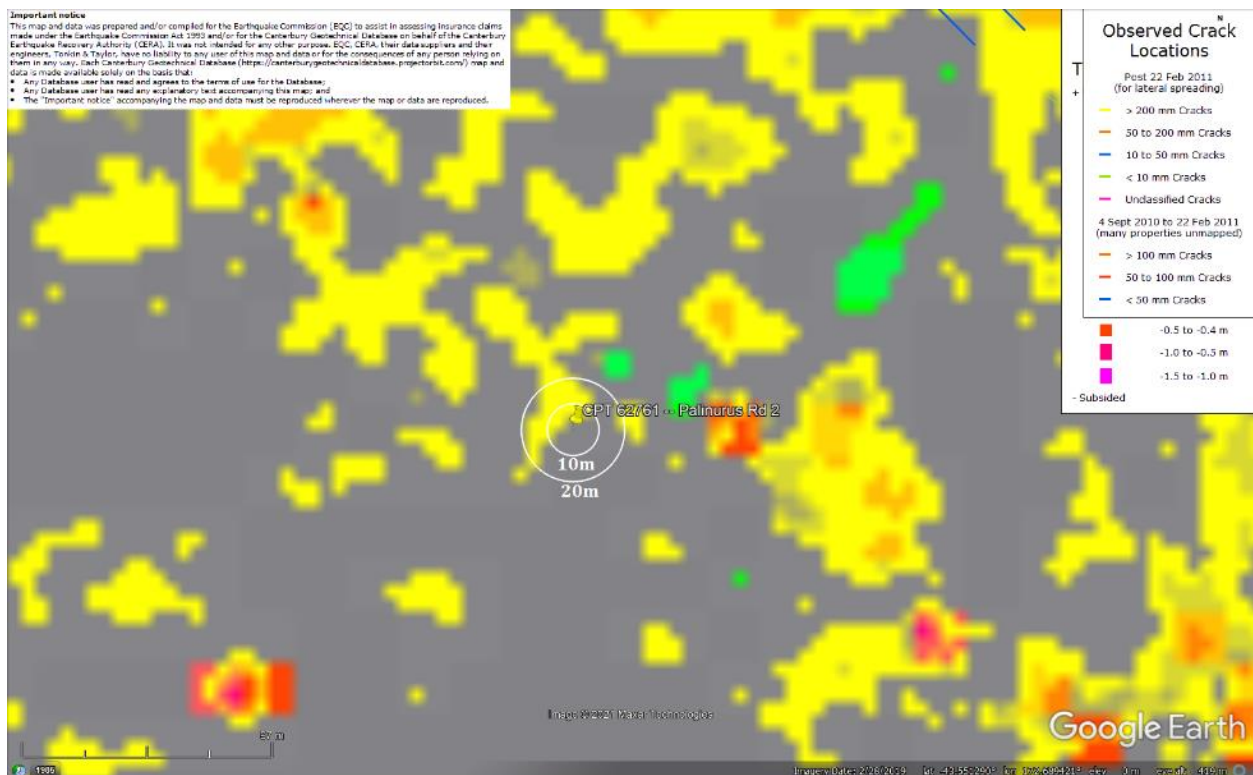


Figure 29: No lateral spreading for Canterbury Earthquake Sequence.

Liquefaction Ejecta Case Histories for 2010-11 Canterbury Earthquakes



Figure 30: Vertical tectonic movements for Sep 2010 Earthquake.

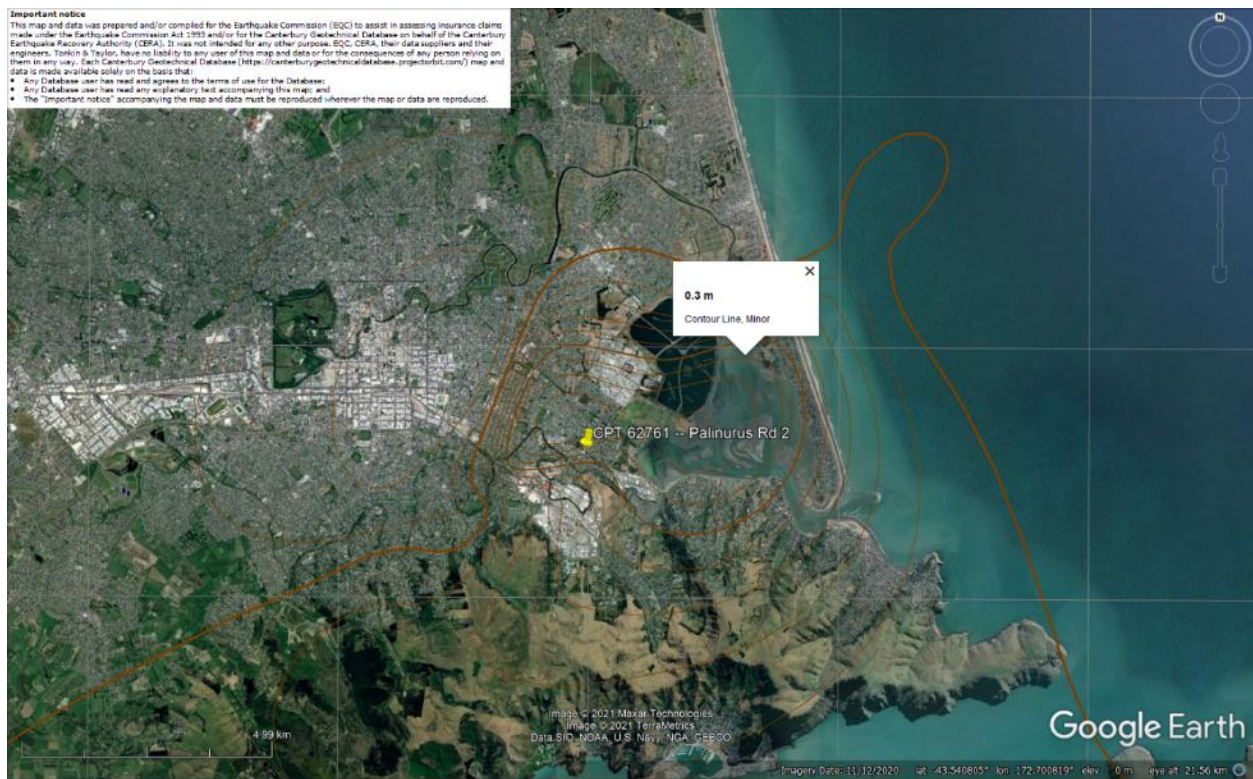


Figure 31: Vertical tectonic movements for Feb 2011 Earthquake.

Liquefaction Ejecta Case Histories for 2010-11 Canterbury Earthquakes



Figure 32: Vertical tectonic movements for June 2011 Earthquake.



Figure 33: Vertical tectonic movements for Dec 2011 Earthquake.

Liquefaction Ejecta Case Histories for 2010-11 Canterbury Earthquakes



Figure 34: Vertical tectonic movements for Canterbury Earthquake Sequence.

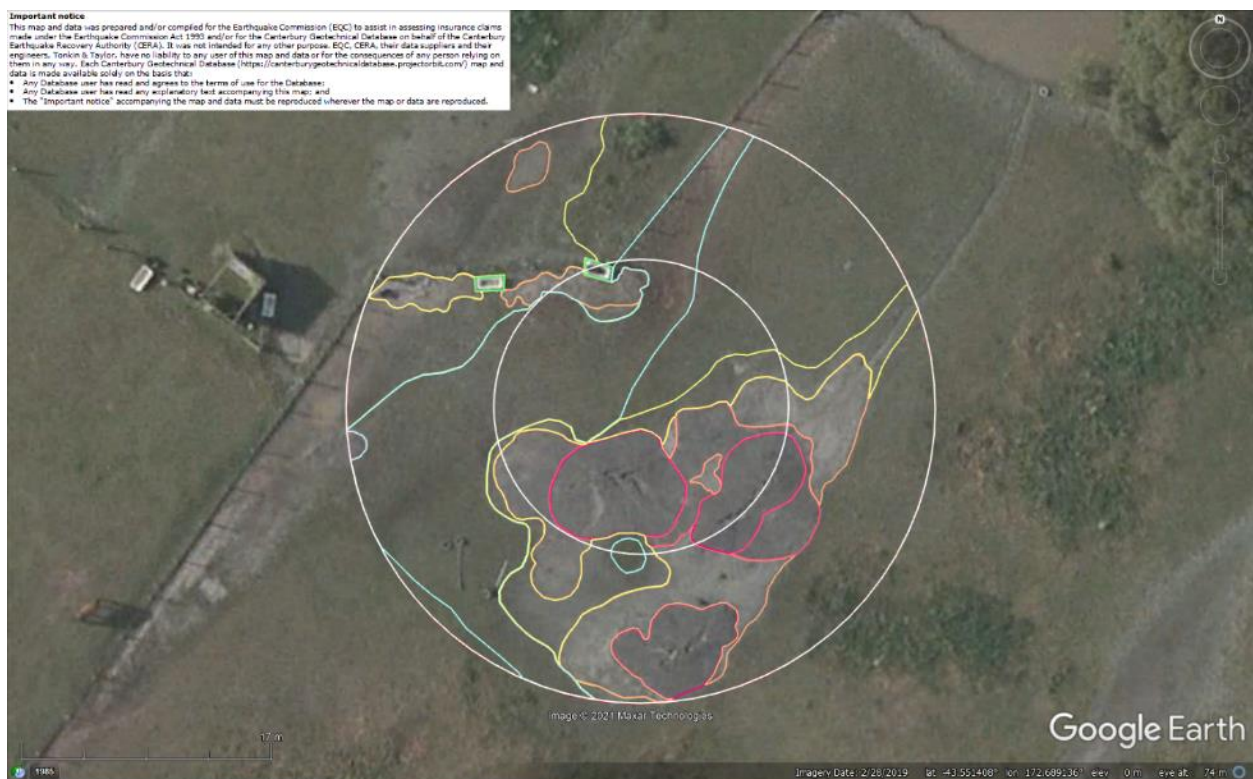


Figure 35: Aerial photograph showing the ejecta outline at the site for Feb-11 EQ.

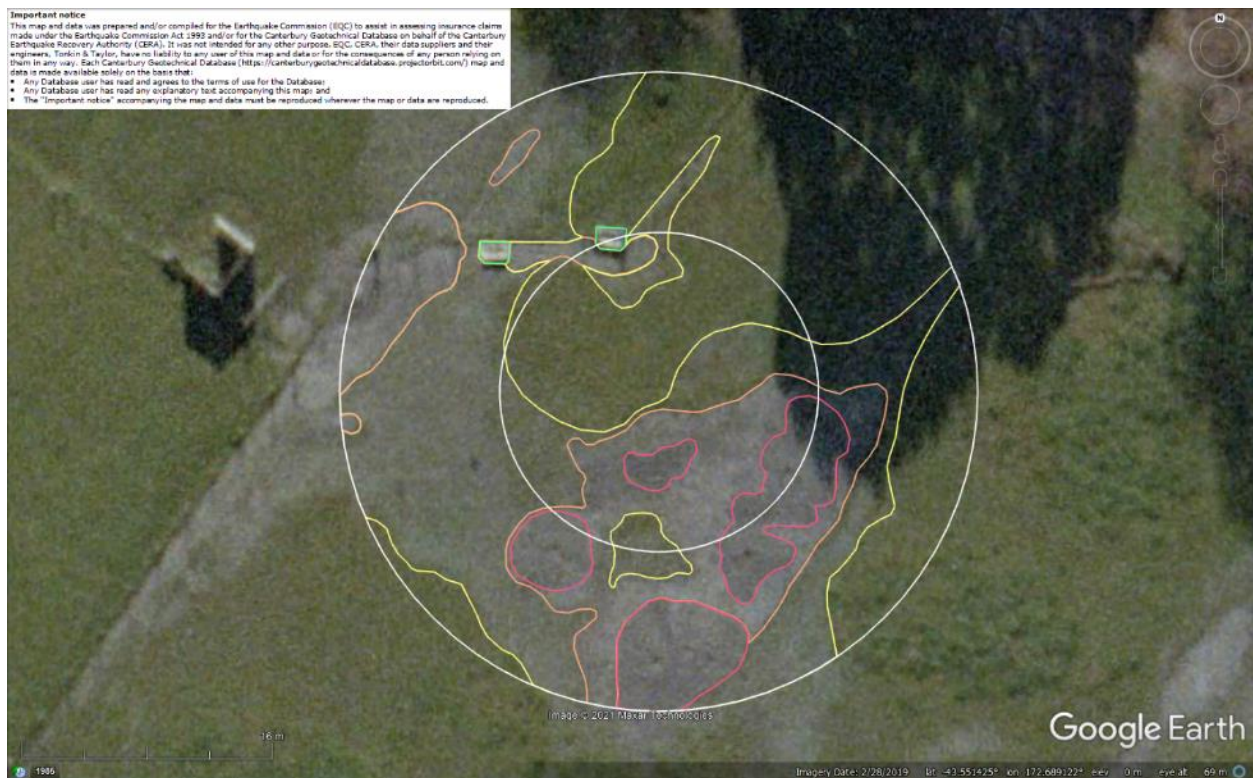


Figure 36: Aerial photograph acquired on 16 Jun 2011 showing the ejecta outline at the site for Jun-11 EQ.

Contents of this figure cannot be shared as doing so is restricted by a Non-Disclosure Agreement.

Figure 37: LDAT inspection notes for a property to the north, outside the 20-m buffer (inspection date: Nov 2011).



Figure 38: Ground photographs showing ejecta remnants at the property to the north, outside the 20-m buffer (photograph date: Nov 2011).

Liquefaction Ejecta Case Histories for 2010-11 Canterbury Earthquakes



Figure 39: Ground photographs showing ejecta remnants just outside the 20-m buffer, toward the southeast (photograph date: Nov 2011).



Figure 40: PGA for Sep-10 EQ (st. dev. = 0.350-0.375 ln units).

Liquefaction Ejecta Case Histories for 2010-11 Canterbury Earthquakes



Figure 41: PGA for Feb-11 EQ (st. dev. = 0.375-0.400 ln units).



Figure 42: PGA for Jun-11 EQ (st. dev. = 0.400-0.425 ln units).

Liquefaction Ejecta Case Histories for 2010-11 Canterbury Earthquakes

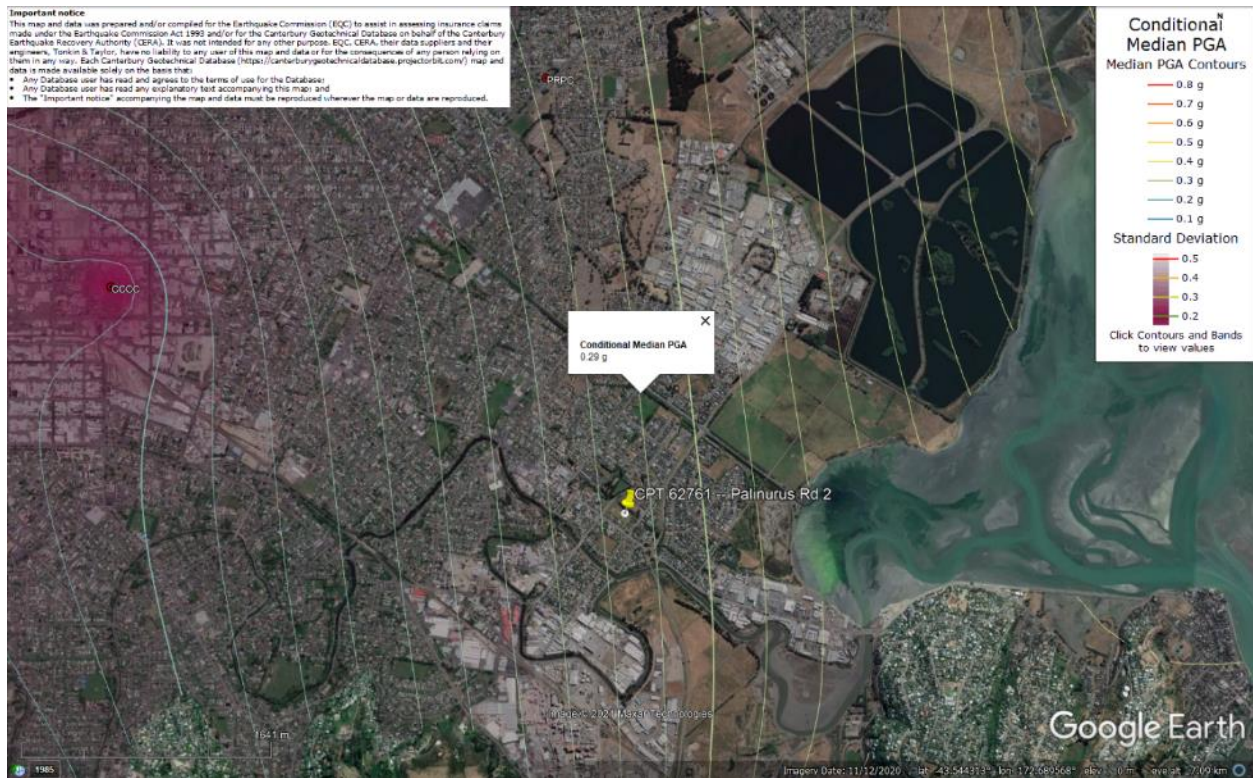


Figure 43: PGA for Dec-11 EQ (st. dev. = 0.425-0.450 ln units).

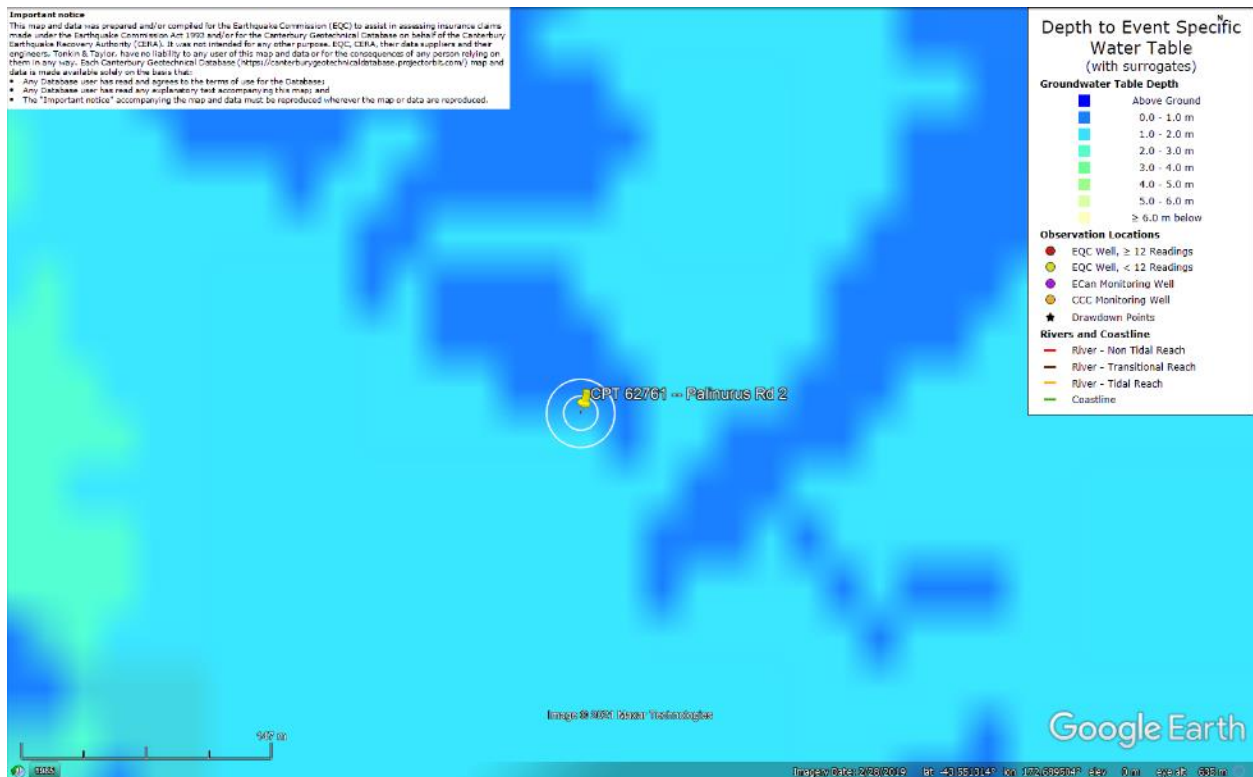


Figure 44: Depth to groundwater table for Sep-10 EQ.

Liquefaction Ejecta Case Histories for 2010-11 Canterbury Earthquakes

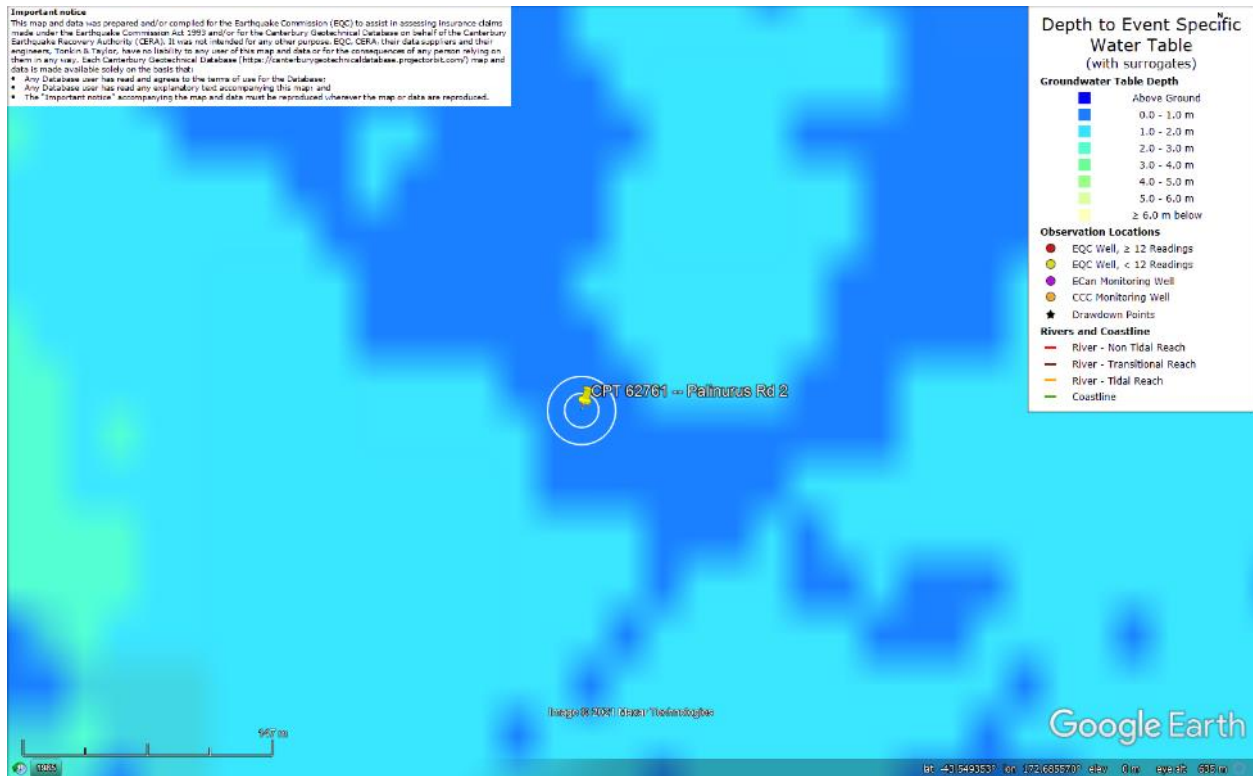


Figure 45: Depth to groundwater table for Feb-11 EQ.

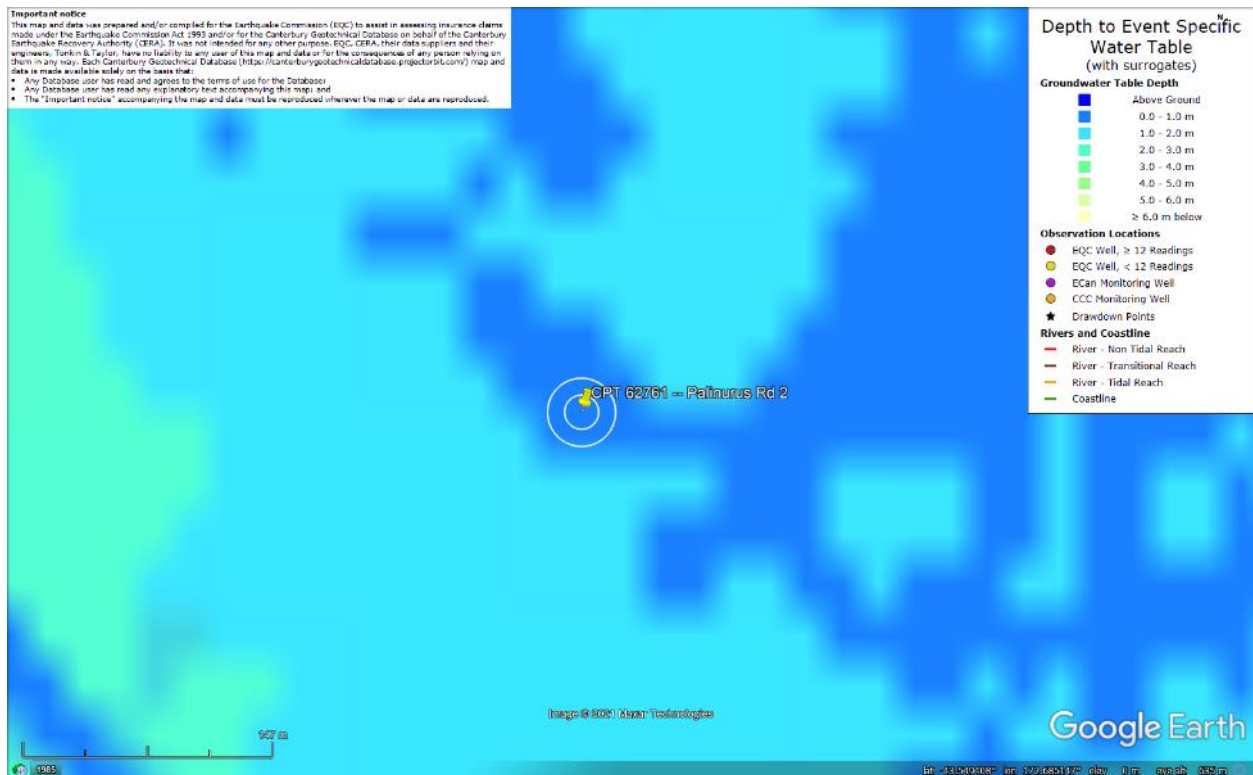


Figure 46: Depth to groundwater table for Jun-11 EQ.

Liquefaction Ejecta Case Histories for 2010-11 Canterbury Earthquakes

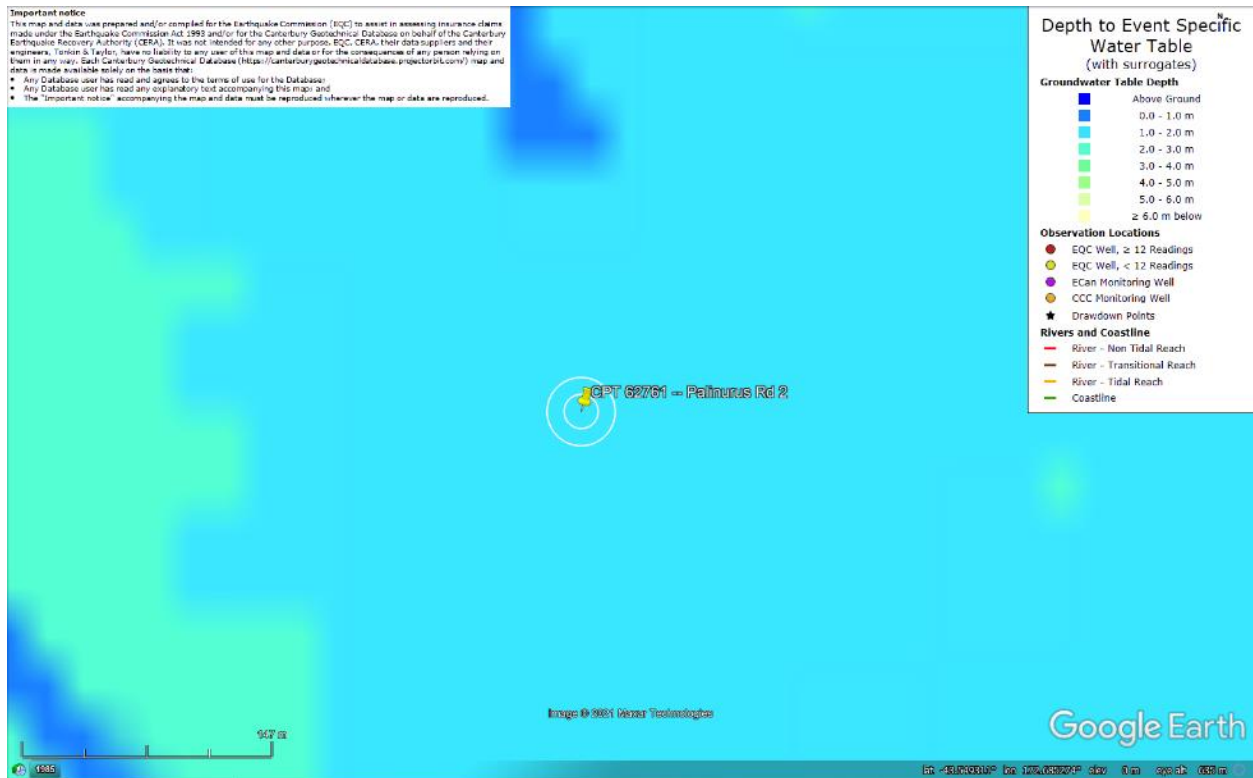


Figure 47: Depth to groundwater table for Dec-11 EQ.

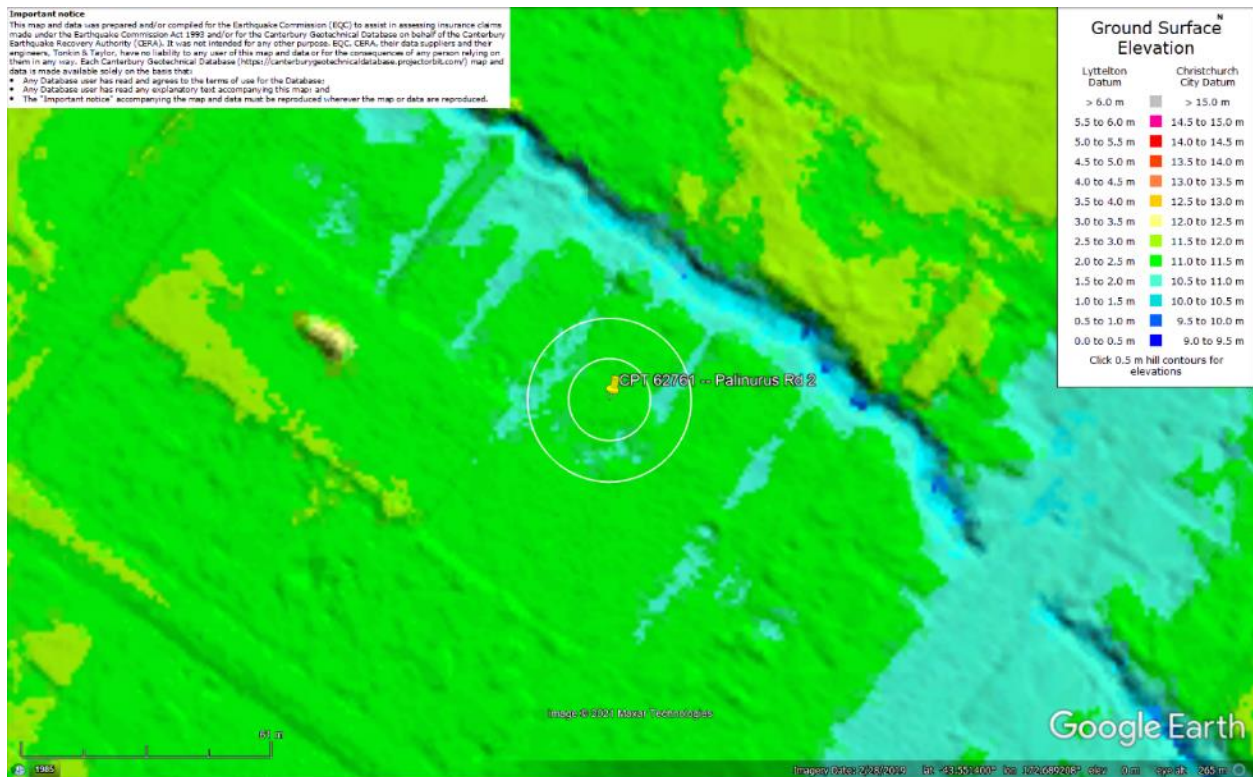


Figure 48: Ground surface elevation according to the Sep-11 LiDAR survey.

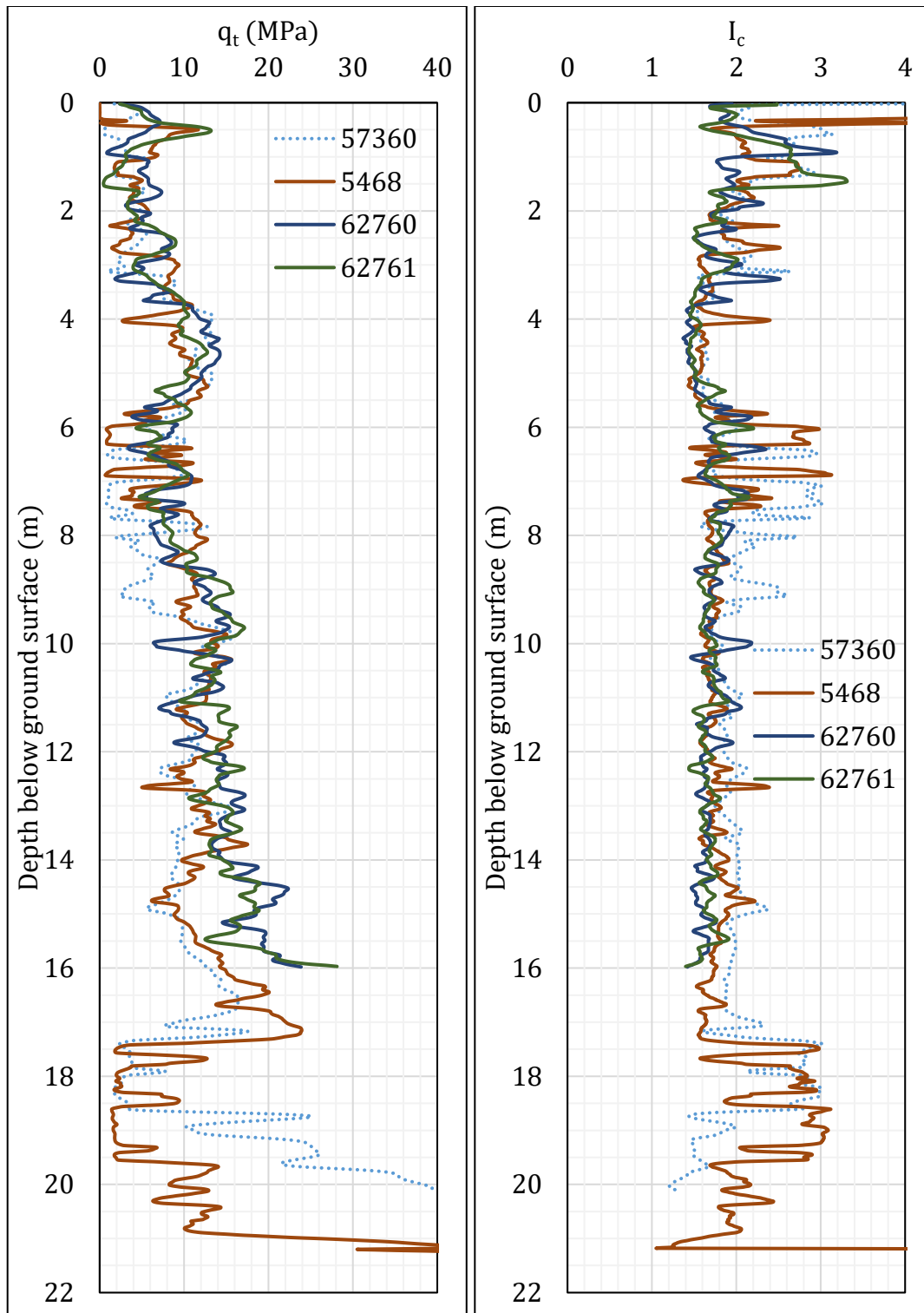


Figure 49: q_t and I_c profiles.

Note 6: The selection of CPTs for the area considered for settlement assessment (Figure 1) is based on the proximity of the CPTs to the considered areas. In accordance with that, the following table shows CPTs that were used for the volumetric settlement analysis in *Cliq v.3.0.3.2*, a CPT soil liquefaction software developed by GeoLogismiki. (The average volumetric settlements were reported in Table 8.)

Table 12: CPT profiles used in volumetric settlement analysis for Patch A selected for settlement assessment.

CPT ID No.	10-m buffer	20-m buffer
62761 (60876)	✓	✓
5468		
62760 (60875)		

Notes: CPT 5468 was used to compute the volumetric settlement for CPTs 62759, 62760, and 62761 for a depth range from 16 m to 20 m; CPT 57360 is located at the center of the Palinurus Rd 1 site.

Table 13a: CPT-based results.

EQ Event	Parameter	CPT ID			
		62761	5468	62760	$\Delta_{16m-20m}$
Sep-10	S _{V1D} (mm)	101	150	99	15
	LSN	22	23	17	1
	LPI	6	7	6	0
	LPI _{ish}	3	3	0	--
	D _{FS<1} (m)	1.56	2.02	3.08	--
Feb-11	S _{V1D} (mm)	239	305	227	30
	LSN	44	49	44	2
	LPI	40	45	38	1
	LPI _{ish}	31	35	29	--
	D _{FS<1} (m)	1.56	1.35	0.98	--
Jun-11	S _{V1D} (mm)	178	250	168	22
	LSN	35	40	31	1
	LPI	20	24	19	0
	LPI _{ish}	15	17	12	--
	D _{FS<1} (m)	1.56	1.49	1.84	--
Dec-11	S _{V1D} (mm)	82	112	81	12
	LSN	19	19	14	1
	LPI	4	5	5	0
	LPI _{ish}	2	2	0	--
	D _{FS<1} (m)	1.56	2.04	3.10	--

Notes: D_{FS<1} = Depth to the first liquefiable layer (FS_L<1) that is at least 200-mm thick, as determined by the Boulanger and Idriss (2016) liquefaction-triggering procedure ($P_L=50\%$, $C_{FC}=0.13$, and $I_{c,cutoff}=2.6$), and exported from *Cliq v.3.0.3.2*; undet. = the specified soil layer was not detected; $\Delta_{17m-20m}$ indicates the amount of S_{V1D}, LSN, and LPI to be added for CPTs 62761 and 62760 due to their penetration depths being shallower than 20 m.

Note 7: Based on the borehole logs (BH 57235, ~75 m to the NW from the center of the site, and BH 6001, ~50 m to the SW from the center of the site) and CPT 62761, the soil profile consists of (1) organic silty, OL, topsoil to a depth of 0.5 m, (2) silt, ML, the Yaldhurst member of the Springston formation, to a depth of 1.6 m, (3) sandy silt, ML, the Yaldhurst member of the Springston formation, to a depth of 2.2 m, (4) fine sand, SP, the Yaldhurst member of the Springston formation, to a depth of 2.7 m, (5) silt, ML, the Yaldhurst member of the Springston formation, to a depth of 3.2 m, (6) fine to medium sand, SP, of the Christchurch formation, to a depth of 17.5 m, (7) sandy silt, ML, of the Christchurch formation, to a depth of 19.5 m, and (8) silty fine sand, SM, of the Christchurch formation, to a depth of 20 m. The groundwater table is at a depth of ~1 m below the ground surface.

Note 8: The Palinurus Rd 2 site had ejecta at the ground surface unlike the Palinurus Rd 1 site, which has a silty soil layer within a depth range from 5.5 m to 9.5 m. This soil layer could have impeded the propagation of excess pore water pressures toward the ground surface and contributed to the absence of liquefaction manifestation at the ground surface of the Palinurus Rd 1 site.

Note 9: The ejecta-induced free-field settlement provided in Table 11 is an areal average settlement due to ejecta, which is based on the total settlement assessment area, A_T (provided in Table 9 and repeated in Table 14). However, the considered area was not always covered completely with ejecta; thus, it is important to provide the localized ejecta-induced settlement, too. The localized settlement due to ejecta is estimated using photographic evidence only as

$$S_{E,P_localized} = \frac{V_E}{A_E}$$

where V_E is the total volume of ejecta within A_T and A_E is the total coverage area of ejecta within A_T . Please note that the areal ejecta-induced settlement provided in Table 14 as S_{E,P_areal} is the same as $S_{E,P}$ in Table 11, which was estimated as

$$S_{E,P_areal} = S_{E,P} = \frac{V_E}{A_T}$$

where V_E is the total volume of ejecta within A_T and A_T is the total settlement assessment area.

Table 14a: Areal and localized ejecta-induced settlement estimates for Patch A (10-m buffer) based on photographic evidence.

Earthquake Event	A_T (m ²)	A_E (m ²)	V_E (m ³)	S_{E,P_areal} (mm)	$S_{E,P_localized}$ (mm)
Sep-10	314	0	0	0	0
Feb-11	313	267	14.4-23.1	60±15	70±15
Jun-11	313	197	6.9-11.1	30±5	45±10
Dec-11	314	0	0	0	0

Notes: $S_{E,P_areal} = S_{E,P}$ reported in Table 11 = areal ejecta-induced settlement; $S_{E,P_localized}$ = localized ejecta-induced settlement; A_T = total settlement assessment area; V_E = total volume of ejecta within A_T ; A_E = total area of ejecta within A_T ; The estimates of both areal and localized ejecta-induced settlement are rounded to the nearest 5; Final plus/minus values are also rounded to the nearest 5.

Table 14b: Areal and localized ejecta-induced settlement estimates for Patch A (20-m buffer) based on photographic evidence.

Earthquake Event	A_T (m ²)	A_E (m ²)	V_E (m ³)	S_{E,P_areal} (mm)	$S_{E,P_localized}$ (mm)
Sep-10	1257	0	0	0	0
Feb-11	1253	868	33.1-54.2	35±10	50±10
Jun-11	1252	816	25.9-42.7	30±5	40±10
Dec-11	1257	0	0	0	0

Notes: S_{E,P_areal} = $S_{E,P}$ reported in Table 11 = areal ejecta-induced settlement; $S_{E,P_localized}$ = localized ejecta-induced settlement; A_T = total settlement assessment area; V_E = total volume of ejecta within A_T ; A_E = total area of ejecta within A_T ; The estimates of both areal and localized ejecta-induced settlement are rounded to the nearest 5; Final plus/minus values are also rounded to the nearest 5.

Summary 2:

The best estimate of the localized ejecta-induced free-field ground settlement at the Palinurus Rd 2 site for the SEP 2010, FEB 2011, JUN 2011, and DEC 2011 earthquake is 0 mm, 50±10 mm, 40±10 mm, and 0 mm, respectively.